Improvement of the photo-Fenton performance at near neutral pH by the addition of tannic acid from tea leaves waste as a complexing agent in the Pb(II) photo-oxidation

Endang Tri Wahyuni*[1], Hardiana Kuncoro[1], Early Zahwa Alharrisa[1], Adhitasari Suratman[1]

Department of Chemistry, Faculty of Mathematic and Natural Sciences,

Gadjah Mada University, Yogyakarta, Indonesia

*) email: endang_triw@ugm.ac.id

Graphical Abstract

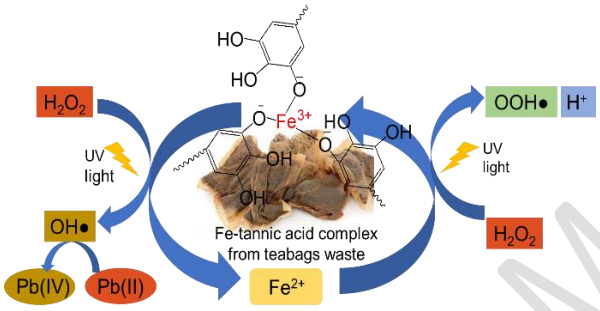

Abstract

Introducing tannic acid from tea leaves waste as a complexing agent of Fe(III) into photo-Fenton process to prevent $Fe(OH)_3$ precipitation at pH 7, and further to increase photo-Fenton activity in the near neutral pH for Pb(II) photo-oxidation is systematically addressed. The photo-Fenton process for Pb(II) photo-oxidation involving Fe^{2+} and H_2O_2 solutions as well as UV light was conducted by batch technique, both in the absence and present of tannic acid. Furthermore, the optimization of tannic acid concentration, solution pH, and reaction time were also conducted. The research results assign that the addition of tannic acid in the photo-Fenton process for photo-oxidation of Pb(II) is able to considerably enhance the effectiveness at pH 6-8 (near neutral pH). The activity of the tannic acid from tea leaves waste is comparable to the that of the commercial tannic acid. The best condition of Pb(II) photo-oxidation having 10 $mg.L^{-1}$ in 50 mL of the solution can be reached by using Fe^{2+} as high 10 $mmol.L^{-1}$, H_2O_2 100 $mmol.L^{-1}$, with the addition of tannic acid as much as 30 $mg.L^{-1}$ at pH 7 and 60 min of the time that gave about 85% of the photo-oxidation effectiveness. It is also indicated that the Pb(II) photo-oxidation has resulted in the harmless PbO_2 solid . Hence, it is obviously assigned that the priceless tea waste could significantly contribute in the improvement of the photo-Fenton performance to prevent environmental pollution.

Key words: Photo-Fenton, near neutral pH, tannic acid, Pb(II) photooxidation.

1. INTRODUCTION

Photo-Fenton is one of the advanced oxidation processes (AOPs) utilizing hydroxyl radical (noted as •OH) as a strong oxidizing agent. The •OH is resulted from the reactions between Fe^{2+} and H_2O_2 as well as UV light with H_2O_2 as presented as equation (1) and (4) below [(Buitrago et al., 2020; Choquehuanca et al., 2021; Ebrahiem et al., 2017a; Miranzadeh et al., 2016; Ortega-Gómez et al., 2012; Saldaña-Flores et al., 2021; Thomas et al., 2021; Wahyuni et al., 2019; Wahyuni et al., 2021):

$Fe^{2+} + H_2O_2 \rightarrow Fe^{3+} + {}^{-}OH + {}^{\bullet}OH$ (1)

$Fe^{3+} + H_2O_2 \rightarrow Fe^{2+} + {}^{\bullet}OOH + H^{+}$ (2)

$Fe^{3+} + {}^{\bullet}OOH \rightarrow H^{+} + O_2 + Fe^{2+}$ (3)

$H_2O_2 + light \rightarrow 2\ {}^{\bullet}OH$ (4)

$Fe^{3+} + {}^{-}OH \rightarrow Fe(OH)_3$ (5)

Due to its easiness, practical and high performance, the method has been intensively examined for photo-degradation of various organic pollutants to form smaller and saver compounds (Ebrahiem et al., 2017a; Miranzadeh et al., 2016)], for photo-oxidation of toxic metal ions such as Pb(II) [(Wahyuni et al., 2019) and As(V) (Wahyuni et al., 2021) to be harmless compounds, as well as for bacterial disinfection (Ortega-Gómez et al., 2012).

Unfortunately, the method works effectively only at pH around 3 or less active in the near neutral pH (Choquehuanca et al., 2021; Ebrahiem et al., 2017b; Miranzadeh et al., 2016; Ortega-Gómez et al., 2012; Saldaña-Flores et al., 2021; Thomas et al., 2021; Wahyuni et al., 2019) due to the precipitate formation of $Fe(OH)_3$ as seen in the Eq. 5. The precipitate can considerably reduce the quantity of Fe^{3+} present and also inhibit the light penetration. These drawbacks constrain the method in the wastewater treatment applications, since most wastewater has pH around 6-8 or near neutral pH (Ebrahiem et al., 2017b; Miralles-Cuevas et al, 2014).

An intensive afford has been demonstrated to extent the method activity in the wider range of pH, that is by introducing a complexing agent (Ahile et al., 2020; Buitrago et al., 2020; De Luca et al., 2014; Fiorentino et al., 2018; Guo et al., 2021; Helal et al., 2013; Miralles-Cuevas et al., 2014; O'Dowd & Pillai, 2020; Pan et al., 2019; Subramanian & Madras, 2016; Villegas-Guzman et al., 2017). The complexing agents are usually organic compounds having several carboxylate groups (Ahile et al., 2020; O'Dowd & Pillai, 2020), including humic acid (Ortega-Gómez et al., 2012), citric acid (Guo et al., 2021; Miralles-Cuevas et al., 2014; O'Dowd & Pillai, 2020; Villegas-Guzman et al., 2017), saccharic acid (Subramanian & Madras, 2016), ethylene diamine tetra acetic acid /EDTA (De Luca et al., 2014; Pan et al., 2019), oxalic acid (De Luca et al., 2014), glutamic acid (Helal et al., 2013), ascorbic acid (Guo et al., 2021; Villegas-Guzman et al., 2017), tartaric acid [(De Luca et al., 2014; Guo et al., 2021; Villegas-Guzman et al., 2017), succinic acid (Guo et al., 2021), caffeic acid (Villegas-Guzman et al., 2017), nitriloacetic acid/NTA (De Luca et al., 2014), (S,S)-ethylenediamine-N,N'-di-succinic acid (EDDS) (Miralles-Cuevas et al., 2014; O'Dowd & Pillai, 2020), and tannic acid (Bolobajev et al., 2016). These complexing agents also named as chelating agents (symbolized as L), are able to react with Fe^{3+} to form Fe-L_3 soluble complex compounds in the wider range pH. Chelation is useful to extend the pH range because the chelating ligand competes favourably with hydroxide ion, for complexes formation that are typically soluble in water (Ahile et al., 2020; O'Dowd & Pillai, 2020). Hence, they can inhibit the precipitate $Fe(OH)_3$ formation, and further enhance the effectiveness of the photo-Fenton process in the near neutral pH.

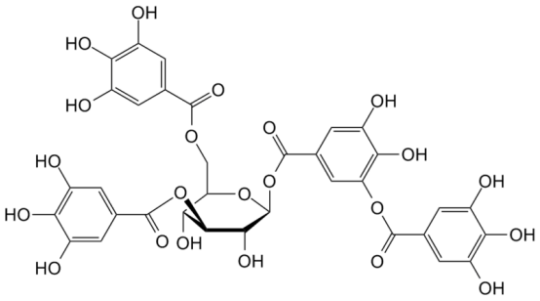

Figure 1. Chemical structure of tannic acid

Another complexing agent is tannic acid, having chemical structure as seen in figure 1. The acid is widely distributed in several plants species such as tea, chocolate, cinnamon, chestnut, and grape, and are also found in wood, bark, leaves and fruit (Baldwin & Booth, 2022). Among them, tea leave waste is one of the priceless sources that has not been explored yet. The use of the tannic acid from very cheap sources will make photo-Fenton a cheaper process, allowing it to be widely applied.

Under the circumstance, in the present research, the addition of tannic acid from the tea leaves waste into conventional photo-Fenton process to increase its activity at the near neutral pH for Pb(II) photo-oxidation is addressed. The subject selected for evaluation of the photo-Fenton modified with tannic acid is Pb(II) ion, since this heavy metal ion is widely dispersed in the water environment due to the disposal of various industrial wastewater (Ebraheim et al., 2022; Wahyuni et al., 2022; Wahyuni et al., 2021). In fact, the heavy metal ion is reported to be hazard for environment and human health (Ebraheim et al., 2022; Pan et al., 2019). Oxidation seems to be the most interesting method for decreasing Pb(II) concentration (Wahyuni et al., 2019), where the harmless and handleable PbO_2 precipitate is resulted (Ebraheim et al., 2022; Wahyuni et al., 2021; Wahyuni et al., 2022). Currently, lack information of the research regarding the Pb(II) photo-oxidation through photo-Fenton process in the presence of tannic acid from the teabag waste is traceable.

Generally, the efficiency of the photo-Fenton process strongly depends on the parameters controlling the process, such as concentrations of Fe^{2+} (Buitrago et al., 2020; De Luca et al., 2014; Helal et al., 2013.; O'Dowd & Pillai, 2020), H_2O_2 (Buitrago et al., 2020; De Luca et al., 2014; Saldaña-Flores et al., 2021), and the complexing agent (De Luca et al., 2014; Miralles-Cuevas et al., 2014), as well as the solution pH (Guo et al., 2021; O'Dowd & Pillai, 2020; Villegas-Guzman et al., 2017; Wahyuni et al., 2019; Wahyuni et al., 2021) and reaction time (Buitrago et al., 2020; Choquehuanca et al., 2021; De Luca et al., 2014; Guo et al., 2021; Helal et al., 2013.; Miralles-Cuevas et al., 2014; O'Dowd & Pillai, 2020; Saldaña-Flores et al., 2021; Villegas-Guzman et al., 2017; Wahyuni et al., 2019; Wahyuni, et al., 2021). Hence, in the present research, the optimal condition of the photo-Fenton process is systematically determined. This study is hoped to valuably contribute to the development of photo-Fenton process and toxic metal remediation technology.

2. EXPERIMENTAL SECTION

2.1. Materials

$FeCl_2$, H_2O_2, commercial tannic acid, and $Pb(NO_3)_2$ purchased from Merck Company were used as received. Waste of teabags was chosen as a source of tannic acid. A set of photo-process apparatus was employed for photo-Fenton process. The analysis instruments including UV-Visible spectrophotometer, atomic absorption spectrophotometer (AAS) and transmission electron microscope equipped with electron diffraction spectrometer (SEM-EDX) machines were operated.

2.2. Research Procedures

Tannic acid extraction from the teabag waste

The teabag waste here is a teabag after being soaked in the hot water for 2 min, which is usually people do to make hot tea. The tea in the teabag waste was taken out from the paper bag and dried in an oven at 80 °C for 1 h. Then the dry tea waste was grounded and sieved into fine powder about 100 μm in size.

The fine powder of the tea waste about 10 g was mixed with 100 mL of ethanol 70%, accompanied by stirring for 18 h to allow the tannic acid dissolved from the tea waste powder into the water media. Then the solution containing tannic acid was separated from the powder by filtration to get a clear solution. It was continued with drying the

clear solution at 80 °C for 1 h, so that the viscous liquid was obtained.

Tannic acid concentration was determined by using UV-Visible spectrophotometer machine. For that purpose, 50 mg of the viscous tannic acid was dissolved in 10 mL ethanol 70% to form clear yellow solution. Then the absorbance of the yellow solution was observed in the range 200-400 nm of the wavelength, which was observed maximally at 295 nm of the wavelength. The concentration was determined by interpolating its absorbance into the respective standard curve. From the calculation, it was found that the content of the tannic acid in the teabag waste was ≈ 42 $mg.g^{-1}$.

Photo-oxidation of Pb(II) by photo-Fenton

Photo-Fenton processes was conducted through batch experiment in the photo-process apparatus that is equipped with 3 UV lamp with 40 watt of each, as illustrated in figure 2. In this typical process, 50 ml of a solution containing Fe^{2+} 10 mmol. L^{-1}, H_2O_2 100 mmol. L^{-1} and Pb (II) 10 $mg.L^{-1}$ was placed in the photo-process apparatus at room temperature, then was irradiated by UV light for a certain period of time. After the desired time, the solution was measured by AAS machine to find the concentration of the Pb(II) left in the solution. The effectiveness of the photo-oxidation (E) is presented as the oxidized Pb(II) in % that is calculated by following equation below:

$$E\ (\%) = \frac{Co - Ct}{Co} \times 100\%$$

Co represents the initial Pb^{2+} concentration ($mg.L^{-1}$) while Ct assigns the concentration of the un-oxidized or the left Pb(II) ($mg.L^{-1}$).

The same procedure was repeated for the processes with various conditions as :
H_2O_2 concentrations were varied as: 25, 50, 75, 100, 125, 150, and 200 mmol. L^{-1} , with Fe^{2+} 10 mmol. L^{-1}, Pb(II) 10 mg. L^{-1} in 50 mL, pH 7, tannic acid 30 mg. L^{-1} and time 60 min.

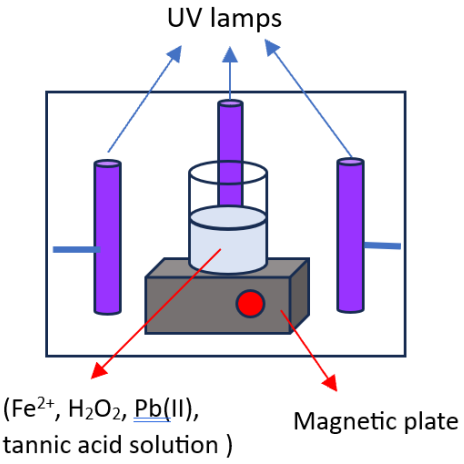

Figure 2. Apparatus for photo-Fenton process

Fe^{2+} concentrations were adjusted as: 2, 4, 6, 8, 10, 12, 14, 16, 18, and 20 mmol. L^{-1}, with H_2O_2 100 mmol. L^{-1}, Pb(II) 10 mg. L^{-1} in 50 mL, pH 7, tannic acid 30 mg. L^{-1} and time 60 min.

The variation of tannic acid concentrations was set as : 10, 20, 30, 40, and 50 mg. L^{-1} with Fe^{2+} 10 mmol. L^{-1}, H_2O_2 100 mmol. L^{-1}, Pb (II) 10 mg. L^{-1} in 50 mL, pH 7, and time 60 min.

The reaction time was altered as : 15, 30, 45, 60, 75, 90, and 150 min, with Fe^{2+} 10 mmol. L^{-1}, H_2O_2 100 mmol. L^{-1}, Pb (II) 10 mg. L^{-1} in 50 mL, pH 7, and tannic acid 30 mg. L^{-1} .

The solution pH was varied as : 1, 3, 5, 7, 9, and 11, with Fe^{2+} 10 mmol. L^{-1}, H_2O_2 100 mmol. L^{-1}, Pb(II) 10 mg. L^{-1} in 50 mL, tannic acid 30 mg. L^{-1} and time 60 min.

3. RESULTS AND DISCUSSION

3.1. Removal of Pb(II) through photo-Fenton process

The Pb(II) ion removal from the aqueous media under photo-Fenton process can be

stimulated by precipitation of insoluble $Pb(OH)_2$, and/or oxidation by •OH provided by Fenton agent and light exposure. The precipitation of Pb^{2+} with ^-OH anionic into $Pb(OH)_2$, written as Eq. 6, can only occur at pH higher than 7.5 assigned by its solubility product constant (Ksp) = $1.43\ 10^{-20}$ (Wahyuni et al., 2022).

$$Pb^{2+} + 2\ ^-OH \rightleftharpoons Pb(OH)_2 \quad (6)$$

$$Pb^{2+} + 2\ \bullet OH \rightarrow PbO_2 + H^+ \quad (7)$$

In fact, the photo-Fenton was conducted at pH 7, suggesting that no precipitation of $Pb(OH)_2$ formed. The second possibility is oxidation by •OH having high oxidation potential, that is 2.8 Volt (Wahyuni et al., 2021; Wahyuni et al., 2022). It is known that the standard reduction potential of Pb(IV)/Pb(II) is −0.67 V (Wahyuni et al., 2022), implying that the reduction is unlikely to proceed. In contrast, with such reduction potential, photo-oxidation of Pb(II) is more favourable. The photo-oxidation of Pb(II) by •OH producing PbO_2 is represented by Eq.7. The more possible oxidation of Pb(II) is in agreement with the study reporting that Pb(II) could be oxidized by chlorine and was accelerated by Mn(VII) (Pan et al., 2019). Accordingly, in the paragraph below, the decrease of the Pb(II) concentration is presented as photo-oxidation degree (in %).

3.2 Effect of the H_2O_2 concentration

In the photo-Fenton process, H_2O_2 is the main reagent to provide •OH both through catalysis decomposition by Fe^{2+}, and simultaneously under UV light exposure, as represented by Eq. 1 and Eq.4 respectively (Ahile et al., 2020; Buitrago et al., 2020; Choquehuanca et al., 2021; De Luca et al., 2014; Ebrahiem et al., 2017b; Fiorentino et al., 2018; Guo et al., 2021; Helal et al., 2013.; Miralles-Cuevas et al., 2014; Miranzadeh et al., 2016; O'Dowd & Pillai, 2020; Ortega-Gómez et al., 2012; Pan et al., 2019; Saldaña-Flores et al., 2021; Subramanian & Madras, 2016; Thomas et al., 2021; Villegas-Guzman et al., 2017; Wahyuni et al., 2019; Wahyuni et al., 2021). The quantity of •OH produced strongly depends on the H_2O_2 concentration (Ahile et al., 2020; Buitrago et al., 2020; O'Dowd & Pillai, 2020), hence it is essential to find the most efficient concentration. Figure 3 exhibits the influence of the H_2O_2 concentration on the Pb(II) photo-oxidation degree.

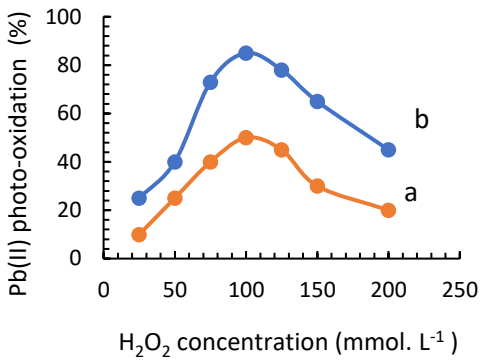

Figure 3. The effect of H_2O_2 concentration, a) in the absent and b) in the present of tannic acid 30 mg.L^{-1}. (Pb(II) : 10 mg.L^{-1} Volume = 50 mL, pH 7, Fe^{2+} = 10 mmol. L^{-1} , time = 60 min).

From figure 3, it is notified that the elevation of H_2O_2 concentration results in the enhancement of the photo-oxidation. The highest level is reached by applying H_2O_2 as much 100 mmol. L^{-1}. However, the higher concentration of H_2O_2 than 100 mmol. L^{-1} is observed to apparently decline the photo-oxidation degree. It is clearly implied that the amount of •OH produced is proportional to the H_2O_2 concentration up to 100 mmol. L^{-1}. A decrease in the photo-oxidation with excessive H_2O_2 occurred because the excess H_2O_2 could capture the •OH present, as seen in Eq. 8 (Buitrago et al., 2020) that forms radical of •OOH. The consecutive reaction of scavenging •OH by the •OOH occurred,

resulting in water and oxygen gas (Eq. 9). These reactions caused the •OH depletion, that was consequently less conductive for the Pb(II) photo- oxidation. The finding trend is well matched with previous reports (Ahile et al., 2020; O'Dowd & Pillai, 2020; Wahyuni et al., 2019; Wahyuni et al., 2021).

$$2H_2O_2 + \bullet OH \rightarrow 2H_2O + \bullet OOH \quad (8)$$

$$\bullet OOH + \bullet OH \rightarrow H_2O + O_2 \quad (9)$$

3.3. Effect of the Fe^{2+} concentration

The role of Fe^{2+} is also very important, that is as a catalyst to promote •OH formation from H_2O_2 decomposition. The amount of •OH produced are also dependent on the quantity of Fe^{2+} ions. Accordingly it is important to get the optimum Fe^{2+} concentration, that was conducted by observing the effect of Fe^{2+} concentration on the Pb(II) photo-oxidation degree.

That result is displayed in figure 4, notifying that the increase of the Fe^{2+} concentration can promote the Pb(II) oxidation which attain the maximum level at 10 mmol. L^{-1} of Fe^{2+} concentration. The extension of Fe^{2+} concentration could generate more •OH, that promoted more effective photo-oxidation. In contrast, the descent photo-oxidation is notified when Fe^{2+} concentration was further elevated into more than 10 mmol. L^{-1}. The excessive Fe^{2+} was able to act as •OH scavenger, as following Eq.10 (Buitrago et al., 2020; Ebrahiem et al., 2017a), that led to the •OH dismissed. Simultaneously, large quantity of Fe^{3+} and ^{-}OH resulted from Eq. 1, were allowed to mutually react to form insoluble $Fe(OH)_3$ (Eq.10). This insoluble hydroxide could screen the light penetration (Ahile et al., 2020; De Luca et al., 2014; O'Dowd & Pillai, 2020; Saldaña-Flores et al., 2021; Wahyuni et al., 2019; Wahyuni et al., 2021). These conditions were less conductive for the photo-oxidation of Pb(II) process. Some others also found same trend data (Ahile et al., 2020; De Luca et al., 2014; O'Dowd & Pillai, 2020; Saldaña-Flores et al., 2021; Wahyuni et al., 2019; Wahyuni et al., 2021).

$$Fe^{2+} + \bullet OH \rightarrow Fe^{3+} + {}^{-}OH \quad (10)$$

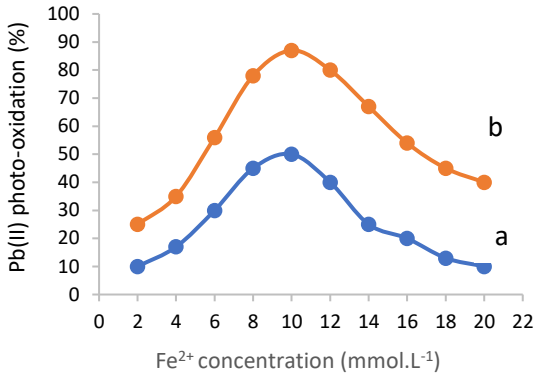

Figure 4. The effect of Fe^{2+} concentration, a) in the absent, and b) in the present of tannic acid (Pb(II) : 10 mg. L^{-1}, volume = 50 mL, pH 7, H_2O_2 = 100 mmol. L^{-1}, time = 60 min).

From the data above, it can be found that the optimal Fe^{2+} concentration is 10 mmol.L^{-1} and for H_2O_2 is 100 mmol. L^{-1}, giving mole ratio of 1/10. It has been frequently reported that the amount of Fe^{2+} was always lower than that of H_2O_2, with the various mole ratio ranging from 1/25 to 1/4 (Buitrago et al., 2020; Ebrahiem et al., 2017a; Wahyuni et al., 2019; Wahyuni et al., 2021). The lesser Fe^{2+} concentration is beneficial in the technical application, since it can inhibit the large amount the production of iron sludge (Buitrago et al., 2020; Ebrahiem et al., 2017a).

3.4. Effect of the tannic acid concentration

Figures 3, 4, 7, and 8 illustrate the effect of the tannic acid addition into the photo-Fenton process. It shows that the addition of tannic acid at pH 7 can distinctly raise the photo-oxidation. The enhancement of the photo-

oxidation is continued to proceed when the tannic acid concentration was raised up to 30 mg. L^{-1}, as depicted in figure 5. In the solution with pH 7, the tannic acid with pKa = 6, is dissociated into its anionic form and hydrogen cation. The anionic tannic acid can easily react with Fe^{3+} ion resulted from the reaction of Fe^{2+} with H_2O_2 (Eq.1.) to form soluble Fe(III)-tannic acid complex compound, as illustrated by figure 6. This formation of the soluble Fe(III)-tannic acid can strongly prevent the formation of insoluble $Fe(OH)_3$ (Bolobajev et al., 2016). Hence, the more tannic anion provided, the more effective prevention of the of $Fe(OH)_3$ formation can be attained.

The contrary photo-oxidation results are notified when the tannic acid concentration was continued to enlarge into larger than 30 mg. L^{-1}. With higher tannic concentration than 30 mg. L^{-1}, there might be free anionic tannic acid that had no chance to react with Fe^{3+}. The free anionic tannic acid was allowed to be degraded by •OH, that dismissed the quantity of the •OH (Bolobajev et al., 2016). Consequently, the photo-oxidation has become less effective (Ahile et al., 2020; Bolobajev et al., 2016; De Luca et al., 2014; O'Dowd & Pillai, 2020).

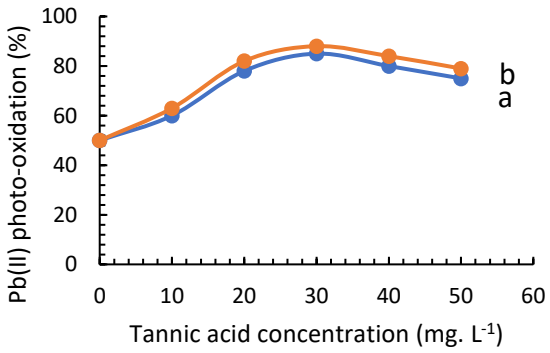

Figure 5. Influence of concentration of the tannic acid: a) from teabag waste, and b) commercial product (Pb(II) = 10 mg.L^{-1}, volume = 50 mL, pH 7, Fe^{2+} = 10 mmol. L^{-1}, H_2O_2 = 100 mmol. L^{-1}, time = 60 min).

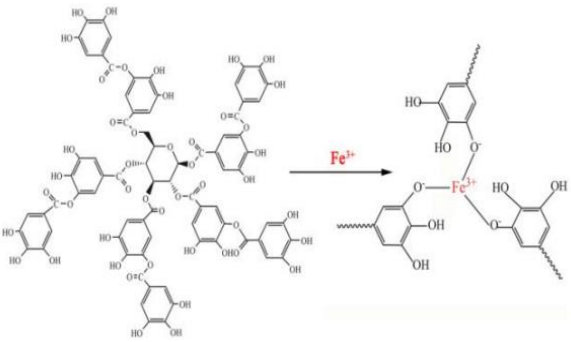

Figure 6. The structure of Fe(III)-tannic complex compound (Bolobajev et al., 2016).

Moreover, it also appears in the figure 5, that the effectiveness of Pb(II) photo-oxidation promoted by tannic acid from teabag waste is seen to be similar, both in trend and effectiveness, to that of by tannic acid commercial. It is evidence that the waste seems to be potential as a cheap and effective chelating agent, that can replace the costly commercial tannic acid .

3.5. Effect of the solution pH

In the photo-Fenton process, pH is a key factor determining the effectiveness of the process. It demonstrates in figure 7, in the process without tannic acid, the photo-oxidation is less effective at very low pH, due to the formation of the stable $Fe(H_2O_2)_2$ complex compound (Ahile et al., 2020; O'Dowd & Pillai, 2020). Such complex formation could neutralize the Fe^{2+} ions, to form inactive catalyst, that prevented the •OH generation (Ahile et al., 2020; O'Dowd & Pillai, 2020). Consequently, the effectiveness of the photo-oxidation was diminished.

It is also notable, the Pb(II) photo-oxidation proceeds more effectively, and reaches the highest level when the pH moves up into 3. In such range pH, the complex of $Fe(H_2O_2)_2$ was dissociated giving more free Fe^{2+} and H_2O_2. The more number of Fe^{2+} and H_2O_2 could stimulate them to mutually react to form large number of •OH, that was conductive for photo-oxidation. The opposite results are shown at pH higher than 3, due to the higher precipitate formation of $Fe(OH)_3$, that filtered the

penetration of light. Consequently, the lesser light was penetrated, leading to the lack of •OH available. This data obtained well agreed with the finding reported by some others (De Luca et al., 2014; Guo et al., 2021; Helal et al., 2013.; Miralles-Cuevas et al., 2014; Villegas-Guzman et al., 2017).

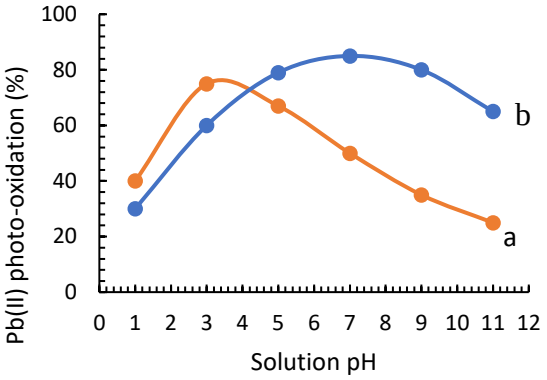

Figure 7. Influence of the solution pH on the photo-oxidation, a) in the absent b) in the present of tannic acid (Pb(II) : 10 mg. L^{-1}, Volume = 50 mL, Fe^{2+} = 10 mmol. L^{-1}, H_2O_2 = 100 mmol. L^{-1}, time = 60 min, tannic acid = 30 mg. L^{-1}).

The figure 7 also assigns clearly that the addition of tannic acid at lower pH, can inhibit the photo-oxidation. In such low pH, tannic acid was formed as non-ionic molecule that is difficult to form complex compounds with Fe^{2+} or Fe^{3+} ions, allowing them to exist as free acid molecules. These free molecules were possible to be degraded by •OH available, that subtracted the radicals present (Bolobajev et al., 2016). The more effective photo-oxidation is observable as the increasing pH from 3 into 7. However, it shows the contrast photo-oxidation results, when the pH was further elevated into higher than 7. In the solution with pH higher than 5, the tannic acid was dissociated into its anions and hydrogen cation, as presented in equation (10) (Bolobajev et al., 2016). The anions are easier to react coordinatively with Fe^{2+} and Fe^{3+} forming soluble complex compound, that could prevent Fe^{3+} from the precipitation with the OH anions present. This condition should maintain the large amount of Fe^{2+} and Fe^{3+} in the solution, that generate more •OH, and finally promoted the higher photo-oxidation. However, at higher pH, the OH anions were formed in excess, that competed with tannic anion in the reaction with Fe^{3+}. Consequently, the number of Fe^{3+} ion was depleted and further declined the photo-oxidation. The similar finding has also been intensively reported (Ahile et al., 2020; Bolobajev et al., 2016; De Luca et al., 2014; Guo et al., 2021; O'Dowd & Pillai, 2020; Villegas-Guzman et al., 2017).

3.6. Effect of the reaction time

Figure 8 represents the alteration time influencing the effectiveness of the photo-oxidation. It is seen in the figure that the prolong reaction time results in the higher photo-oxidation and the photo-oxidation kept to increase as the reaction time was further lengthen up to 60 min. The photo-oxidation is not depended on the time after 60 minutes of the reaction. The longer reaction time, the more OH radicals could be provided and the more effective contact between the OH radicals with Pb^{2+} ions also proceeded. After 60 mins, more PbO_2 solids may be formed in the solution that prevented the light entering into the solution (Wahyuni et al., 2019). Consequently, the photo-oxidation insignificantly was altered or even slightly went down. This data is in a good agreement with other reports (Wahyuni et al., 2019; Wahyuni et al., 2021).

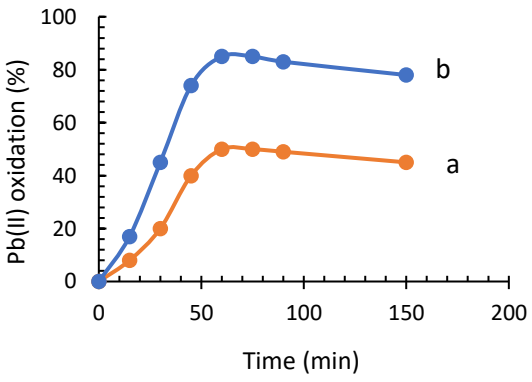

Figure 8. Influence of the reaction time on the photo-oxidation, a) in the absent and b) in the present of tannic acid (Pb(II): 10 mg.L^{-1}, Volume = 50 mL, Fe^{2+} = 10 mg.L^{-1}, H_2O_2 = 100 mg.L^{-1}, pH = 7, tannic acid = 30 mg.L^{-1}).

3.7. Detection of the iron and Pb(IV) present after the photo-Fenton process

It has been reported that the Pb(II) photo-oxidation has produced PbO_2 solid material (Wahyuni et al., 2019; Wahyuni et al., 2021). In order to confirm the formation of the oxide, SEM image accompanied with the EDX spectra have been taken. Figure 8 depicts the result of SEM and EDX spectra of slurry material from photo-Fenton process. From the EDX spectra, it is notable the presence of Fe and Pb elements. The presence of Fe element was originated from the insoluble $Fe(OH)_3$ whereas the Pb element may be attributed to PbO_2. From the EDX spectra, it is obviously implied that the oxidation has resulted in PbO_2.

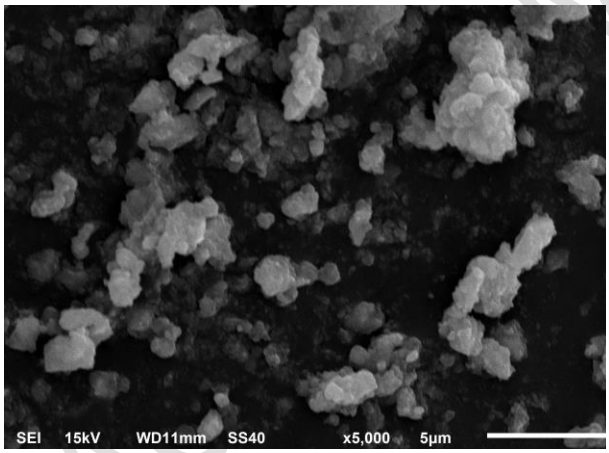

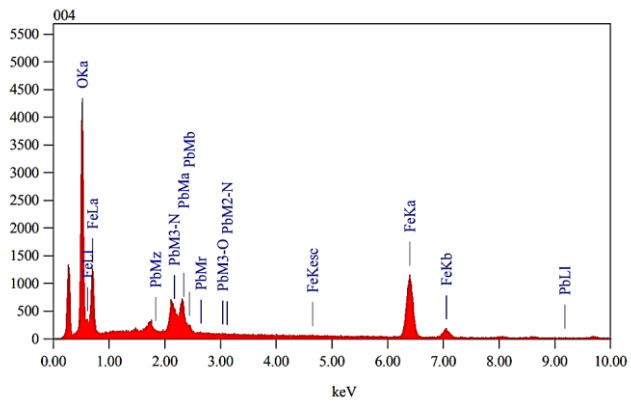

Figure 9. The SEM image and EDX spectra of the slurry from the photo-Fenton process.

To find the content of Pb in more quantitatively, X-ray fluorescence (XRF) analysis was conducted and the results from the photo-Fenton process with various tannic acid concentration were exhibited in Table 1.

Table 1. Elemental composition of the slurry from photo-Fenton in the Pb(II) photo-oxidatio conducted by XRF.

Tannic acid addition (mg.L^{-1})	Pb(II) photo-oxidation from the solution (%)	Pb content from slurry (% mol)	Fe content from slurry (% mol)
10	60.25	6.26	12.52
30	85.50	15.74	7.70
50	75.12	10.52	9.80

It is notable from the table that the content of Pb appears to increase, while the Fe amount decreases, This data is consistent with the degree of the Pb(II) photo-oxidation. The data provides clearly evidence that the photo-oxidation of Pb(II) into PbO_2 was successfully proceeded.

CONCLUSION

It is concluded that the addition of tannic acid from the teabag waste into the photo-Fenton process can considerably enhance the process performance at the near neutral pH in the Pb(II) photo-oxidation. Furthermore, the enhancement of the photo-oxidation result is found to be controlled by tannic acid concentration, and the tannic acid as much 30 mg.L^{-1} showed the highest effect in the improvement. The ability of the tannic acid from the teabag waste is found to be comparable with the commercial tannic acid. In addition, the highest photo-oxidation of 100 mL of Pb(II) 10 mg. L^{-1}, about 86%, can be achieved by employing Fe^{2+} 10 mmol. L^{-1}, H_2O_2

100 mmol. L^{-1}, pH 7 and time 60 min in the presence of 30 mg.L^{-1} tannic acid. Hence, it is beneficial from the utilizing the priceless waste to enhance photo-Fenton performance in the reducing the toxic contaminant.

REFERENCES

Ahile, U. J., Wuana, R. A., Itodo, A. U., Sha'Ato, R., & Dantas, R. F. (2020). A review on the use of chelating agents as an alternative to promote photo-Fenton at neutral pH: Current trends, knowledge gap and future studies. In Science of the Total Environment (Vol. 710). Elsevier B.V. https://doi.org/10.1016/j.scitotenv.2019.134872

Baldwin, A., & Booth, B. W. (2022). Biomedical applications of tannic acid. In Journal of Biomaterials Applications (Vol. 36, Issue 8, pp. 1503–1523). SAGE Publications Ltd. https://doi.org/10.1177/08853282211058099

Bolobajev, J., Trapido, M., & Goi, A. (2016). Interaction of tannic acid with ferric iron to assist 2,4,6-trichlorophenol catalytic decomposition and reuse of ferric sludge as a source of iron catalyst in Fenton-based treatment. Applied Catalysis B: Environmental, 187, 75–82. https://doi.org/10.1016/j.apcatb.2016.01.015

Buitrago, J. L., Sanabria, J., Gútierrez-Zapata, H. M., Urbano-Ceron, F. J., García-Barco, A., Osorio-Vargas, P., & Rengifo-Herrera, J. A. (2020). Photo-Fenton process at natural conditions of pH, iron, ions, and humic acids for degradation of diuron and amoxicillin. Environmental Science and Pollution Research, 27(2), 1608–1624. https://doi.org/10.1007/s11356-019-06700-y

Choquehuanca, A., Ruiz-Montoya, J. G., & La Rosa-Toro Gómez, A. (2021). Discoloration of methylene blue at neutral pH by heterogeneous photo-Fenton-like reactions using crystalline and amorphous iron oxides. Open Chemistry, 19(1), 1009–1020. https://doi.org/10.1515/chem-2021-0077

De Luca, A., Dantas, R. F., & Esplugas, S. (2014). Assessment of iron chelates efficiency forphoto-Fenton at neutral pH. Water Research, 61, 232–242. https://doi.org/10.1016/j.watres.2014.05.033

Ebraheim, G., Karbassi, A. R., & Mehrdadi, N. (2022). Employing speciation of metals to assess photo-assisted electrochemical efficiency for improving rainwater quality in Tehran, Iran. International Journal of Environmental Science and Technology, 19(1), 261–280. https://doi.org/10.1007/s13762-021-03127-2

Ebrahiem, E. E., Al-Maghrabi, M. N., & Mobarki, A. R. (2017a). Removal of organic pollutants from industrial wastewater by applying photo-Fenton oxidation technology. Arabian Journal of Chemistry, 10, S1674–S1679.https://doi.org/10.1016/j.arabjc.2013.06.012

Ebrahiem, E. E., Al-Maghrabi, M. N., & Mobarki, A. R. (2017b). Removal of organic pollutants from industrial wastewater by applying photo-Fenton oxidation technology. Arabian Journal of Chemistry, 10, S1674–S1679. https://doi.org/10.1016/j.arabjc.2013.06.012

Fiorentino, A., Cucciniello, R., Di Cesare, A., Fontaneto, D., Prete, P., Rizzo, L., Corno, G., & Proto, A. (2018). Disinfection of urban wastewater by a new photo-Fenton like process using Cu-iminodisuccinic acid complex as catalyst at neutral pH. Water Research, 146, 206–215. https://doi.org/10.1016/j.watres.2018.08.024

Guo, Q., Zhu, W., Yang, D., Wang, X., Li, Y., Gong, C., Yan, J., Zhai, J., Gao, X., & Luo, Y. (2021). A green solar photo-Fenton process for the degradation of carbamazepine using natural pyrite and organic acid with in-situ generated H_2O_2. Science of the Total Environment, 784.

https://doi.org/10.1016/j.scitotenv.2021.147187

Helal, M., Ali, O., & Hussein Mady, A. (2013). Catalytic Degradation of Phenol Using Different Chelating Agents at Near Neutral pH in Modified-Fenton process Anti-inflammatory heterocyclic Steroids View project wastewater treatment using modified Fenton reaction as applicable method View project. https://www.researchgate.net/publication/282750928

Miralles-Cuevas, S., Oller, I., Pérez, J. A. S., & Malato, S. (2014). Removal of pharmaceuticals from MWTP effluent by nanofiltration and solar photo-Fenton using two different iron complexes at neutral pH. Water Research, 64, 23–31. https://doi.org/10.1016/j.watres.2014.06.032

Miranzadeh, M. B., Zarjam, R., Dehghani, R., Haghighi, M., Badi, H. Z., Marzaleh, M. A., & Tehrani, A. M. (2016). Comparison of fenton and photo-fenton processes for removal of linear alkyle benzene sulfonate (LAS) from aqueous solutions. Polish Journal of Environmental Studies, 25(4), 1639–1648. https://doi.org/10.15244/pjoes/61824

O'Dowd, K., & Pillai, S. C. (2020). Photo-Fenton disinfection at near neutral pH: Process, parameter optimization and recent advances. In Journal of Environmental Chemical Engineering (Vol. 8, Issue 5). Elsevier Ltd. https://doi.org/10.1016/j.jece.2020.104063

Ortega-Gómez, E., Fernández-Ibáñez, P., Ballesteros Martín, M. M., Polo-López, M. I., Esteban García, B., & Sánchez Pérez, J. A. (2012). Water disinfection using photo-Fenton: Effect of temperature on Enterococcus faecalis survival. Water Research, 46(18), 6154–6162. https://doi.org/10.1016/j.watres.2012.09.007

Pan, W., Pan, C., Bae, Y., & Giammar, D. (2019). Role of Manganese in Accelerating the Oxidation of Pb(II) Carbonate Solids to Pb(IV) Oxide at Drinking Water Conditions. Environmental Science and Technology, 53(12), 6699–6707. https://doi.org/10.1021/acs.est.8b07356

Pan, Y., Guo, H., Zhou, M., Zhang, Y., Tian, Y., & Wang, W. (2019). EDTA enhanced removal of sulfamethazine by pre-magnetized Fe_0 without oxidant addition. Chemical Engineering Journal, 372, 905–916. https://doi.org/10.1016/j.cej.2019.04.211

Saldaña-Flores, K. E., Flores-Estrella, R. A., Alcaraz-Gonzalez, V., Carissimi, E., de Souza, B. G., Ruotolo, L. A. M., & Urquieta-Gonzalez, E. (2021). Regulation of hydrogen peroxide dosage in a heterogeneous photo-fenton process. Processes, 9(12). https://doi.org/10.3390/pr9122167

Subramanian, G., & Madras, G. (2016). Introducing saccharic acid as an efficient iron chelate to enhance photo-Fenton degradation of organic contaminants. Water Research, 104, 168–177. https://doi.org/10.1016/j.watres.2016.07.070

Thomas, N., Dionysiou, D. D., & Pillai, S. C. (2021). Heterogeneous Fenton catalysts: A review of recent advances. In Journal of Hazardous Materials (Vol. 404). Elsevier B.V. https://doi.org/10.1016/j.jhazmat.2020.124082

Villegas-Guzman, P., Giannakis, S., Torres-Palma, R. A., & Pulgarin, C. (2017). Remarkable enhancement of bacterial inactivation in wastewater through promotion of solar photo-Fenton at near-neutral pH by natural organic acids. Applied Catalysis B: Environmental, 205, 219–227. https://doi.org/10.1016/j.apcatb.2016.12.021

Wahyuni, E. T., Nurhikmatillah, A., Kurniasari, H., & Siswanta, D. (2021). Detoxification of As(III) in aqueous media by using photo-Fenton method. Global Nest Journal, 23(4), 550–555. https://doi.org/10.30955/gnj.003265

Wahyuni, E. T., Pratama, N. A., Lestari, N. D., & Suherman, S. (2022). Enhancement of

TiO_2 activity under visible light by N,S codoping for Pb(II) removal from water. Journal of Engineering and Applied Science, 69(1). https://doi.org/10.1186/s44147-022-00069-5

Wahyuni, E. T., Rahmaniati, T., Hafidzah, A. R., Suherman, S., & Suratman, A. (2021). Photocatalysis over N-doped TiO_2 driven by visible light for Pb(II) removal from aqueous media. Catalysts, 11(8). https://doi.org/10.3390/catal11080945

Wahyuni, E. T., Siswanta, D., Kunarti, E. S., Supraba, D., & Budiraharjo, S. (2019). Removal of Pb(II) ions in the aqueous solution by photo-Fenton method. Global Nest Journal, 21(2), 180–186. https://doi.org/10.30955/gnj.002936